

Motor-Independent Targeting of CLASPs to Kinetochores by CENP-E Promotes Microtubule Turnover and Poleward Flux

Stefano Maffini,¹ Ana R.R. Maia,¹ Amity L. Manning,^{2,3} Zoltan Maliga,⁴ Ana L. Pereira,^{1,5} Magno Junqueira,⁴ Andrej Shevchenko,⁴ Anthony Hyman,⁴ John R. Yates III,⁶ Niels Galjart,⁵ Duane A. Compton,^{2,3} and Helder Maiato^{1,7,*}

¹Instituto de Biologia Molecular e Celular, Universidade do Porto, Rua do Campo Alegre 823, 4150-180 Porto, Portugal

²Department of Biochemistry, Dartmouth Medical School, Hanover, NH 03755, USA

³Norris Cotton Cancer Center, Dartmouth-Hitchcock Medical Center, Lebanon, NH 03766, USA

⁴Max Planck Institute for Molecular Cell Biology and Genetics, 01307 Dresden, Germany

⁵Department of Cell Biology and Department of Genetics, Erasmus MC Rotterdam, 3000 CA Rotterdam, The Netherlands

⁶Department of Chemical Physiology, The Scripps Research Institute, 10550 North Torrey Pines Road, SR11, La Jolla, CA 92037, USA

⁷Laboratory of Cell and Molecular Biology, Faculdade de Medicina, Universidade do Porto, 4200-319 Porto, Portugal

Summary

Efficient chromosome segregation during mitosis relies on the coordinated activity of molecular motors with proteins that regulate kinetochore attachments to dynamic spindle microtubules [1]. CLASPs are conserved kinetochore- and microtubule-associated proteins encoded by two paralog genes, *clasp1* and *clasp2*, and have been previously implicated in the regulation of kinetochore microtubule dynamics [2–4]. However, it remains unknown how CLASPs work in concert with other proteins to form a functional kinetochore microtubule interface. Here we have identified mitotic interactors of human CLASP1 via a proteomic approach. Among these, the microtubule plus-end-directed motor CENP-E [5] was found to form a complex with CLASP1 that colocalizes to multiple structures of the mitotic apparatus in human cells. We found that CENP-E recruits both CLASP1 and CLASP2 to kinetochores independently of its motor activity or the presence of microtubules. Depletion of CLASPs or CENP-E by RNA interference in human cells causes a significant and comparable reduction of kinetochore microtubule poleward flux and turnover rates and rescues spindle bipolarity in Kif2a-depleted cells. We conclude that CENP-E integrates two critical functions that are important for accurate chromosome movement and spindle architecture: one relying directly on its motor activity, and the other involving the targeting of key microtubule regulators to kinetochores.

Results and Discussion

To shed light on the molecular context of human CLASPs during mitosis, we identified CLASP1-interacting proteins from nocodazole-arrested HeLa cells stably expressing localization affinity purification (LAP)-tagged CLASP1 [4]. LAP

purification [6] followed by mass spectrometry analysis recovered known CLASP1 interactors in mammals, such as CLIP-170, LL5 β , GCC185, and astrin [7–9] (A.L.M., S.F. Bakhom, S.M., C.C. Melo, H.M., and D.A.C., unpublished data). Additionally, we identified CENP-E in our human CLASP1 purification, confirming previous results obtained in *Xenopus* meiotic egg extracts [10]. This approach also identified novel candidate CLASP1 binding partners, including the centriolar proteins CENP-J/CPAP and ninein [11, 12], as well as MARK kinases [13] (Figure 1A).

Of the full list of CLASP1 interactors (see Table S1 available online), CENP-E is the only bona fide kinetochore (KT) protein [14]. Importantly, the functional significance of the CLASP1/CENP-E interaction remains unknown, and it was therefore selected for in-depth analysis. We started by using mass spectrometry to confirm that endogenous CLASP1 copurifies with CENP-E (Figure 1A). Notably, endogenous CLASP2 was also found in the purification, suggesting that CENP-E forms distinct complexes with CLASP1 and CLASP2 (Figure 1A). The reciprocal interaction of human CLASP1 with CENP-E was confirmed by western blot after immunoprecipitation with anti-green fluorescent protein (GFP) antibodies in nocodazole-arrested HeLa cells stably expressing GFP-CLASP1 or CENP-E-GFP (Figure 1B). Finally, immunofluorescence analysis showed that endogenous CLASP1 and CENP-E colocalize to multiple structures of the mitotic apparatus throughout mitosis, including centrosomes, KTs, and the spindle midzone and midbody (Figure S1). Altogether, these data suggest that CLASPs and CENP-E might be involved in functionally related aspects of mitosis.

Previous work in *C. elegans*, an organism lacking CENP-E orthologs, has shown that the CENP-F-like proteins HCP-1 and HCP-2 recruit CLASP to KTs [15]. However, as opposed to in *C. elegans*, CENP-F depletion in human cells apparently does not affect CLASP1 KT recruitment [16]. In order to test whether CENP-E could fulfill the task of targeting CLASPs to KTs in human cells, we depleted ~80% of CENP-E from HeLa cells (Figure S2), which led to a significant reduction of CLASP1 (~80%; n luciferase RNAi = 387 KTs from 18 cells; n CENP-E RNAi = 579 KTs from 15 cells; p < 0.001 by Mann-Whitney test) and CLASP2 (~65%; n luciferase RNAi = 332 KTs from 10 cells; n CENP-E RNAi = 321 KTs from 10 cells; p < 0.001 by Mann-Whitney test) KT levels in a microtubule (MT)-independent manner (Figures 2A, 2B, and 2F; Figures S3 and S4). Importantly, CLASP1 and CLASP2 localization in the spindle and centrosomes was not affected by CENP-E depletion (Figure 2B; Figure S4; data not shown). On the contrary, depletion of both CLASPs from HeLa cells by RNAi (~90% depletion; Figures S2 and S6) caused no measurable change in CENP-E localization at KTs (n luciferase RNAi = 350 KTs from 9 cells; n CLASPs-RNAi = 348 KTs from 8 cells; p = 0.438 by Mann-Whitney test) regardless of the presence of MTs (Figure 2C; Figures S3 and S6). Under these conditions, CLASP1 was completely removed from KTs, but a detectable RNAi-resistant pool of stable protein remained associated with structures at spindle poles resembling centrioles (Figure 2C) [4]. Overall, these results indicate that CENP-E is required to specifically target a significant pool of CLASP1 and CLASP2 to KTs.

*Correspondence: maiato@ibmc.up.pt

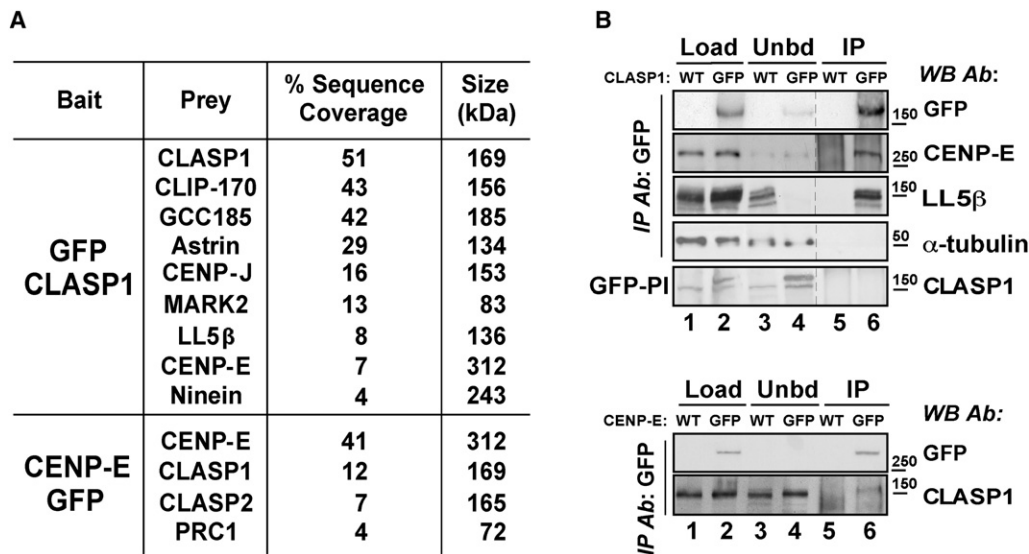


Figure 1. Human CLASP1 Interacts with CENP-E

(A) Mass spectrometry analysis of affinity purified GFP-(LAP)-CLASP1 and CENP-E-GFP identifies novel protein interactions. Polypeptides identified (Prey) and the percentages of the relative sequence coverage are indicated. A complete list of the polypeptides identified during this analysis is shown in Table S1. (B) Anti-GFP immunoprecipitation from mitotic enriched HeLa cells stably expressing GFP-(LAP)-CLASP1 or CENP-E-GFP. Native protein extracts (Load) obtained from the indicated cell lines, unbound proteins (Unbd), and immunoprecipitations (IP) were subjected to western blotting with the indicated antibodies. Immunoprecipitations were blotted for LL5 β and α -tubulin as positive and negative controls. Immunoprecipitations performed with anti-GFP pre-immunization serum (GFP-PI) as precipitating antibody were analyzed by western blotting with rabbit anti-CLASP1 antibody. Quantification of CENP-E levels in the GFP-CLASP1 immunoprecipitation revealed a 131% increase relative to control. Quantification of CLASP1 levels in the CENP-E-GFP immunoprecipitation revealed a 135% increase relative to control.

The MT independence of CENP-E-mediated targeting of CLASPs to KTs makes it unlikely to rely on the MT plus-end-directed motor activity of CENP-E. To directly test this prediction, we quantified CLASP1 KT levels in HeLa cells overexpressing a motorless CENP-E construct (GFP-CENP-E N Δ 803), which causes a dominant-negative effect by preventing endogenous CENP-E from assembling onto KTs [17] and recruits CLASP1 to many cytoplasmic aggregates (Figure S5). Under these conditions, CLASP1 KT levels were similar to non-transfected control cells (Figures 2D and 2F; n nontransfected = 322 KTs from 8 cells; n transfected = 308 KTs from 8 cells). To confirm these results, we used a recently identified fluorenone, UA62784, reported to inhibit CENP-E ATPase activity but not its KT localization [18]. HeLa cells treated with 100 nM UA62784 for 12 hr showed normal CENP-E and CLASP1 localization at KTs (Figures 2E and 2F; Figure S3; n control = 314 KTs from 8 cells; n UA62784-treated = 299 KTs from 8 cells). Overall, these results lead to two conclusions: (1) the CENP-E motor domain is not required for interaction with CLASP1, and (2) recruitment of CLASP1 to KTs is a novel motor-independent function of CENP-E.

One remarkable feature of KTs is their capacity to constantly renew their MT composition (i.e., KT MT turnover) while allowing the poleward translocation (i.e., flux) of attached MTs [19]. This is critical to ensure proper chromosome segregation and genomic stability by preventing the formation of incorrect KT MT attachments [20, 21]. Studies in *Drosophila melanogaster* culture cells have shown that the single *clasp* ortholog in this organism is required for the poleward translocation of MT subunits within KT MTs [3]. To dissect the functional significance of the interaction between CLASPs and CENP-E in this process, we used pulses from a 405 nm laser to photoactivate GFP- α -tubulin stably expressed in human U2OS cells

and measured the velocity at which the fluorescent mark activated in the proximity of chromosomes approached the pole. Consistent with previous reports [22], in control cells at late prometaphase/metaphase, the fluorescent mark approached the pole with a mean velocity of $0.53 \pm 0.18 \mu\text{m}/\text{min}$ (Figure 3A; Table 1; Movie S1), with cells entering anaphase with normal kinetics after photoactivation (data not shown). In contrast, after RNAi depletion of $\sim 90\%$ of CLASP1 or both CLASPs (Figure S2), the fluorescent mark approached the pole at $0.36 \pm 0.09 \mu\text{m}/\text{min}$ and $0.26 \pm 0.10 \mu\text{m}/\text{min}$, respectively (Figure 3B; Table 1; Movie S1). Depletion of $\sim 80\%$ of CENP-E by RNAi (Figure S2D) phenocopies the simultaneous depletion of both CLASPs, with the fluorescent mark approaching the pole at $0.27 \pm 0.11 \mu\text{m}/\text{min}$ (Figure 3C; Table 1; Movie S1). In a small subset of experiments, we were successful in marking both half-spindles and noted a similar reduction in the rates at which fluorescent marks on opposing KT MTs moved apart after CLASP or CENP-E RNAi in comparison with controls (Table 1). Altogether, these results suggest that flux rates in human cells are sensitive to the KT levels of CLASP1 and CLASP2, which are largely determined by CENP-E. Curiously, loss of function of the single *clasp* ortholog in *Drosophila* causes bipolar spindles to gradually collapse into monopolar spindles as a result of continuous depolymerization of MTs at their minus ends, whereas tubulin subunit incorporation at the plus ends is attenuated [3, 23]. This scenario is somewhat different from our knockdown of CLASPs (or CENP-E) in human cells, where spindles were 20%–30% shorter than control cells in prometaphase or metaphase (n luciferase RNAi = 29; n CLASP RNAi = 28; n CENP-E RNAi = 13; $p < 0.001$ by t test) but only rarely formed monopolar spindles (Figure 3D; unpublished data; [24]). However, anti-CLASP1 antibody injections in HeLa cells do cause the formation of

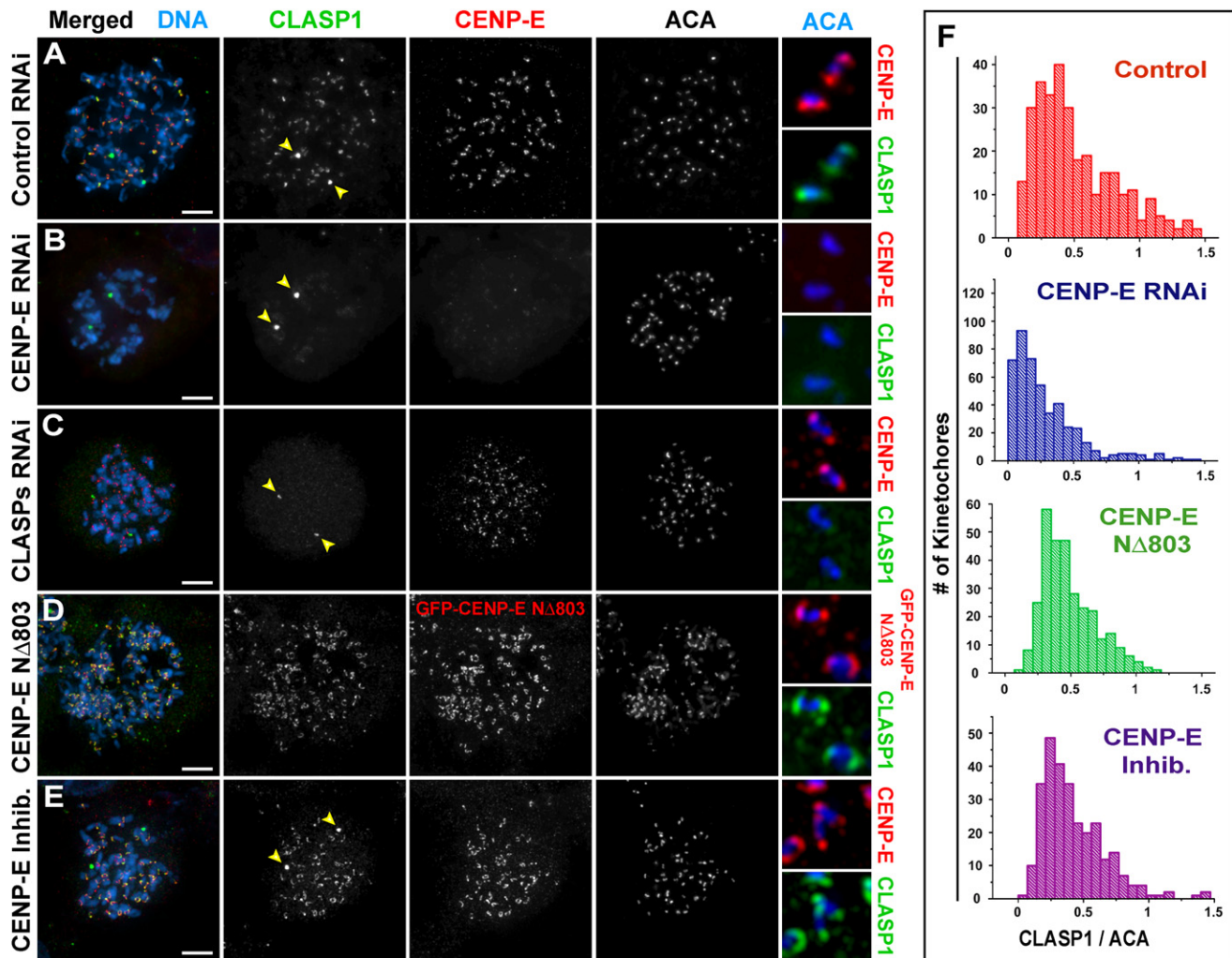


Figure 2. CENP-E Targets CLASP1 to Kinetochores in a Motor-Independent Manner

(A–E) For each cell, a magnification of an area containing kinetochores (KTs; colored as indicated) is shown in the smaller panels at right. Arrowheads indicate centrosomes; scale bars represent 5 μ m.

(A–C) Interdependency analysis of CLASP1 and CENP-E localization. HeLa cells treated with the indicated specific siRNAs were prepared for chromosome spreads in the presence of 10 μ M nocodazole to fully depolymerize microtubules (MTs). Following fixation, cells were stained for endogenous CLASP1 and CENP-E. ACA was used as an inner-KT marker, and DNA was stained with DAPI.

(D and E) The dependency of CLASP1 KT targeting from the motor domain of CENP-E was tested in HeLa cells transfected with a construct overexpressing a dominant-negative motorless GFP-CENP-E (GFP-CENP-E N Δ 803) (D) or in HeLa cells treated with UA62784 (E), an inhibitor of CENP-E ATPase activity. Cells were prepared for chromosome spreads, fixed, and stained for CLASP1 (D) or CLASP1 and CENP-E (E).

(F) Quantification of CLASP1/ACA KT fluorescence ratio in control cells (A), CENP-E RNAi cells (B), cells transfected with GFP-CENP-E N Δ 803 (D), or cells treated with UA62784 (E).

monopolar spindles [2], suggesting that some residual function of CLASPs after RNAi is still sufficient to prevent the full collapse of the spindle while allowing some poleward MT flux.

We also determined how CLASPs and CENP-E affect KT MT turnover by measuring fluorescence loss on the photoactivated area over time, after background subtraction and photo-bleaching correction, and fitting the results to a double exponential curve [19–21, 25]. The fast-decay component was interpreted to represent non-KT MTs that rapidly lose their activated fluorescence, whereas the slower-decay component likely corresponds to the more stable KT MTs in which the activated fluorescence is more persistent (Figure 3E). Surprisingly, the calculated half-time turnover for KT MTs in cells depleted for CLASPs or CENP-E was significantly higher (396.5 ± 48 s, $n = 8$, $p < 0.001$ and 317.3 ± 35.2 s, $n = 13$, $p < 0.025$,

respectively) than in control cells (155.2 ± 13.9 s, $n = 14$) (Figures 3E and 3F; Figure S2), suggesting increased KT MT stability. Previous studies in mammalian cells lacking CENP-E or microinjected with function-blocking antibodies have shown 23%–50% reduction in MT binding at KT, which has been interpreted as indicating that CENP-E is required to stabilize KT MT attachments [26, 27]. However, depletion of CENP-E or CLASPs in HeLa cells did not prevent the formation of cold-stable KT MTs (Figure S7), indicating that despite a reduction in the number of KT MTs, these are actually more stably attached, possibly through point contacts with core KMN (KNL1/MIS12/NDC80) components [28], but the capacity to recruit new MTs might be impaired. Importantly, the half-time turnover observed for non-KT MTs in control (16 ± 1.2 s), CLASP-depleted (11.9 ± 0.9 s), and CENP-E-depleted

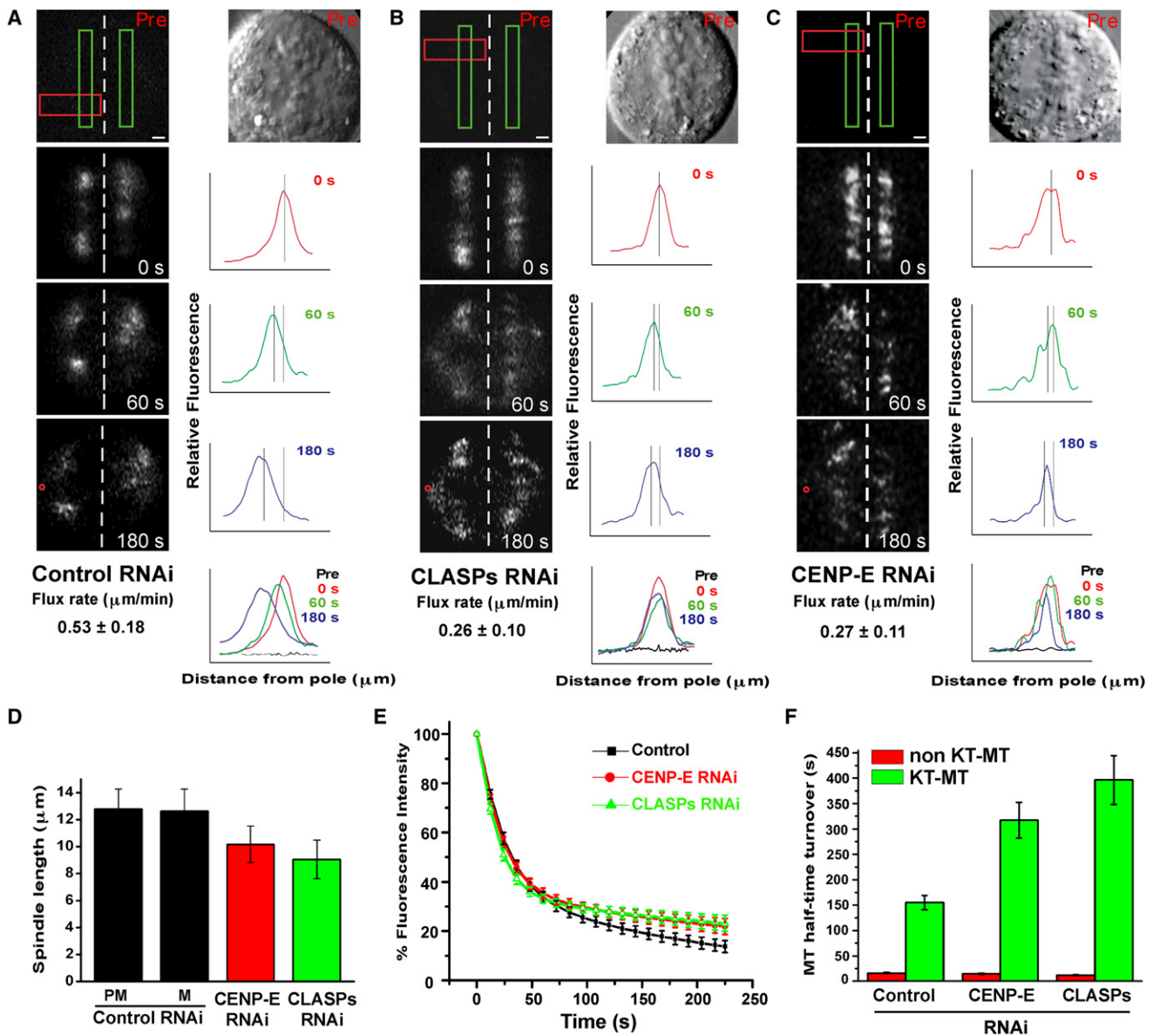


Figure 3. CENP-E Targeting of CLASPs to KTs Is Required to Sustain Normal Kinetochores Microtubule Dynamics

(A–C) Human U2OS cells in late prometaphase/metaphase depleted for CLASPs or CENP-E display a significant reduction of KT MT poleward flux. Metaphase cells were identified by differential interference contrast and imaged (Pre); fluorescence images were captured before (Pre) and at various times (indicated in seconds) after photoactivation of GFP- α -tubulin with pulses from a 405 nm laser in one or two areas of the spindle (green rectangles). Line scans represent the relative fluorescence intensity of individual KT MTs in a defined area (red rectangle) of the fluorescence images. Lines indicate the position of peak fluorescence intensity; flux rates were determined by plotting the position of peak fluorescence intensity as a function of time. Red circles indicate the position of spindle poles. Scale bars represent 1 μm .

(D) Cells deficient for CENP-E or CLASPs exhibit shorter spindles (PM, prometaphase; M, metaphase). Data are presented as the mean \pm standard deviation.

(E) Cells depleted for CENP-E or CLASPs show a significantly higher KT MT half-time turnover. Normalized fluorescence intensity over time after photoactivation of U2OS cells (in late PM/M) following treatment with the indicated siRNA is shown. Data are presented as the mean \pm standard error of the mean corrected for background subtraction and photobleaching.

(F) Calculated MT half-time turnover for U2OS cells in (E). Data are presented as the mean \pm standard error of the mean.

(14.6 ± 1.2 s) cells was similar, indicating that the contribution of these proteins to non-KT MT turnover is minor. Thus, CENP-E-mediated targeting of CLASPs to KTs enables attached MTs to exchange more rapidly and become less stable overall. Interestingly, both CLASPs and CENP-E levels at KTs decrease as cells progress from prometaphase to anaphase [2, 4, 29], consistent with the observation that KT MTs become

less dynamic at anaphase onset [19]. CLASPs may render KT MTs less stable by recruiting the kinesin-13 MT depolymerase Kif2b to KTs, thereby promoting high MT turnover as cells progress into metaphase [21, 30]. Alternatively, the affinity of CLASPs to MTs may decrease when cells enter mitosis, altering the balance with MT depolymerases and favoring KT MT destabilization. Interestingly, it has recently been reported

Table 1. Poleward Microtubule Flux Rates in Photoactivatable GFP- α -Tubulin U2OS Cells

	Control	CLASP1 RNAi	CLASP RNAi	CENP-E RNAi
Mark to pole (μ m/min)	0.53 \pm 0.18 (28)	0.36 \pm 0.09 (8; <0.001)	0.26 \pm 0.10 (19; <0.001)	0.27 \pm 0.11 (13; <0.001)
Mark away from mark on opposing KT MTs/2 (μ m/min)	0.53 \pm 0.07 (3)	0.26 \pm 0.07 (4; <0.001)	0.28 \pm 0.15 (3; 0.002)	0.23 \pm 0.02 (3; 0.002)

Values show mean \pm standard deviation; n and p versus control are given in parentheses.

that TOGp, a member of a widely conserved protein family commonly viewed as MT stabilizers, also acts to destabilize spindle MTs during mitosis [31].

Depletion of Kif2a by RNAi in U2OS cells leads to the formation of monopolar spindles, and bipolarity can be rescued with treatments that either disrupt the formation of KT MTs or render them less dynamic [21, 32]. In order to investigate whether CLASPs and CENP-E at KTs work in concert in the same molecular pathway required for spindle architecture, we compared the efficiency of bipolar spindle formation after codepleting CLASPs or CENP-E with Kif2a by RNAi (Figure S8). Depletion of CLASP1 or both CLASPs in U2OS cells was sufficient to rescue spindle bipolarity in ~80% of Kif2a-deficient cells while maintaining KT MTs (Figure S8; unpublished data). This is likely because of a relatively low contribution of CLASP2 during mitosis in U2OS cells as compared to HeLa cells [24]. Interestingly, a functional cooperation between CLASP and the kinesin-13 protein KLP10A has been previously observed in *Drosophila* S2 cells [33, 34], suggesting evolutionary conservation of spindle architecture in both systems. Finally, CENP-E depletion rescued spindle bipolarity in Kif2a-deficient cells in 85% of the cases (Figure S8), confirming that CLASPs and CENP-E at KTs work in the same pathway involved in spindle formation and maintenance.

Based on in vitro studies, it has been proposed that CENP-E tethers KTs to dynamic MTs independently of its ATPase activity [35]. Based on our functional data, this property of CENP-E can be explained in vivo by a novel motor-independent role in targeting CLASPs to KTs, thereby contributing to establish and/or maintain functional KT MT attachments. It is noteworthy that perturbation of CLASP function does not produce persistent mono-oriented chromosomes as in many cells following CENP-E inhibition [5, 17, 26, 36]. This suggests that there are some unique activities of CENP-E that are not fulfilled by CLASPs. In this context, we propose that CENP-E integrates at least two activities. One is the powering of chromosome alignment (through its kinesin motor activity) by sliding on preexisting spindle MTs [36], a function that is somewhat independent of CLASPs. The second function of CENP-E is to recruit CLASPs to KTs to functionally modulate KT MT dynamics, which explains why KT MT flux and turnover change if either CENP-E or CLASPs are lost. On the basis of the more complex spindle phenotype associated with CLASP depletion in HeLa cells, there might be other CLASP-interacting proteins involved in centriole and spindle function found in this study that do not interact with CENP-E (unpublished data). Finally, the results presented here challenge current models for how CENP-E communicates with the spindle assembly checkpoint (SAC) [37–39]. According to these models, CENP-E has been proposed to be important for the capture and stabilization of MTs at KTs, thereby contributing to SAC silencing. In light of the data presented here indicating that CENP-E promotes destabilization rather than stabilization of MT attachments, alternative models must be put forward. An attractive one might involve the participation of CENP-E in destabilizing

erroneous KT MT attachments under control of Aurora B [20] while antagonizing the MT-stabilizing role of BubR1 [40, 41]. Because Aurora B controls the targeting of BubR1, CENP-E, and Kif2b to KTs [21, 42], it is possible that CLASPs are also important players under regulation by this pathway to make mitosis error-free [4].

Experimental Procedures

Cell Culture, RNAi, Drug Treatments, Transfections, and Western Blotting

Human HeLa, HeLa LAP-CLASP1 [4], HeLa CENP-E-GFP [43], and U2OS-PA-GFP- α -tubulin [22] cells were grown in Dulbecco's modified Eagle's medium at 37°C in the presence of 5% CO₂ and supplemented with 10% fetal bovine serum and antibiotics. Human CLASP1, CLASP2, CENP-E, Kif2a, and Nuf2 levels were reduced with specific small interfering RNA (siRNA) oligonucleotides as described previously [24, 32, 44, 45] (A.L.M., S.F. Bakhoun, S.M., C.C. Melo, H.M., and D.A.C., unpublished data). Phenotypes were analyzed and quantified 48 hr and 72 hr after RNAi treatment, and protein depletion was monitored by western blot with the following antibodies: rabbit anti-CLASP1 1:1000 [46], rat anti-CLASP1 1:200 and rabbit anti-CENP-E 1:500 (Santa Cruz), rabbit anti-Kif2a 1:500 [32], rabbit anti-Eg5 1:500 (A.L.M., S.F. Bakhoun, S.M., C.C. Melo, H.M., and D.A.C., unpublished data), and mouse anti- α -tubulin 1:2000 (Sigma). HRP-conjugated secondary antibodies (Amersham) were visualized via the ECL system (Pierce). To enrich HeLa LAP-CLASP1 or HeLa CENP-E-GFP cell cultures for mitotic cells for mass spectrometry and immunoprecipitation analyses, 100 ng/ml or 5 ng/ml nocodazole, respectively, was added to the media for 16 or 18 hr before harvesting. For inhibition of CENP-E ATPase activity, 100 nM UA62784 was added to the media for 12 hr before analysis [18]. For photobleaching correction in the MT half-time turnover experiments, control cells were treated with 5 μ M paclitaxel 10 min before starting imaging. Transfection of HeLa cells with GFP-CENP-E NA803 was performed as described previously [2] and analyzed 48 hr after transfection. Wild-type and *clasp2* KO mouse embryonic fibroblasts were grown as described previously [4].

Immunofluorescence

HeLa and U2OS cells were processed for immunofluorescence as described previously [2, 32]. Primary antibodies used were rabbit anti-CLASP1 1:300 [2]; sheep anti-CENP-E 1:500 (gift from W. Earnshaw, University of Edinburgh); rat anti-CLASP1 1:100, rat anti-CLASP2 1:100, and rabbit anti-CENP-E 1:300 (Santa Cruz); human anti-ACA 1:1000 (gift from W. Earnshaw); and mouse anti- α -tubulin 1:2000 (Sigma). Immunofluorescence on chromosome spreads was performed as described previously [2]. Secondary antibodies used were Alexa 488, 568, and 647 1:2000 (Invitrogen, Molecular Probes), and DNA was counterstained with DAPI (1 μ g/ml). For cold-induced MT depolymerization experiments, HeLa cells were incubated 15 min on ice and 1 min with 0.2% Triton X-100 in PHEM buffer (60 mM PIPES, 25 mM HEPES, 10 mM EGTA, 2 mM MgCl₂). After a 30 min fixation in 4% paraformaldehyde in PHEM buffer followed by 5 min methanol postfixation, cells were processed for immunofluorescence as described above.

Mass Spectrometry and Immunoprecipitation

Native protein extracts from HeLa LAP-CLASP1 [4] or HeLa CENP-E-GFP [43] cell cultures enriched for mitotic cells by nocodazole treatment were prepared for mass spectrometry analysis as described previously [6, 47]. The presented list of CLASP1-interacting proteins was filtered for known common contaminants in LAP purifications. Immunoprecipitation (IP) experiments were performed with aliquots of native protein extracts (3 mg of total protein in a total volume of 500 μ l of IP buffer: 150 mM KCl, 75 mM HEPES [pH 7.5], 1.5 mM EGTA, 1.5 mM MgCl₂, 10% glycerol, 0.1% NP40,

and protease inhibitors) prepared from HeLa LAP-CLASP1 or HeLa CENP-E-GFP cell cultures enriched for mitotic cells by incubation with nocodazole. Protein extracts were incubated with the precipitating antibody at 4°C for 4 hr on a rotating platform. Precipitating primary antibodies used were rabbit anti-GFP 1:100 and rabbit anti-GFP preimmunization serum (GFP-PI) 1:100. These extracts were then incubated with 40 μ l of protein A Sepharose for 2 hr at 4°C on a rotating platform. Samples were centrifuged, the supernatant was retained as unbound sample, and the pelleted beads were washed three times with washing buffer (IP buffer with 250 mM KCl). Precipitated proteins were removed from the beads by boiling for 5 min in SDS sample buffer and subjected to electrophoresis followed by western blot with the appropriate antibody: rabbit anti-GFP 1:1000 and rabbit anti-CENP-E 1:100 (Santa Cruz), anti-LL5 β 1:2000 (gift from A. Akhmanova, Erasmus MC Rotterdam), anti- α -tubulin 1:2000 (Sigma), and rabbit anti-CLASP1 1:1000 [46].

Fluorescence Quantification at KTs

Protein accumulation at KTs of HeLa cells prepared for chromosome spreads and immunostained with rat anti-CLASP1 or rat anti-CLASP2, rabbit anti-CENP-E, and human anti-ACA was measured for individual KTs by quantification of the pixel gray levels of the focused z plane within a region of interest (ROI). Background was measured outside the ROI and subtracted from the measured fluorescence intensity inside the ROI. Results were normalized against a constitutive KT marker (ACA) with a custom routine written in MATLAB.

GFP- α -Tubulin Photoactivation Analysis

For photoactivation studies, mitotic human U2OS cells stably expressing photoactivatable GFP- α -tubulin [22] were identified by differential interference contrast microscopy. After acquisition of a preactivation frame, two 0.8 s pulses from a 405 nm laser were used to activate GFP- α -tubulin in one or two areas of $\sim 7 \mu\text{m}^2$ inside the spindle. Imaging was performed with a Leica SP2 spectral confocal microscope with a 63 \times /1.4 NA objective lens with an additional 7 \times zoom; images were acquired every 3 s during the first 4 min and subsequently every 30 s. For MT poleward flux experiments, quantification of fluorescence intensity of the activated areas and quantification of flux rates were performed as described previously [22]. Quantification of MT half-time turnover was performed as described previously [19–21, 25], where the background-subtracted fluorescence values of an activated area were corrected for photobleaching by determining the fluorescence loss in activated spindles from paclitaxel-treated cells. The fluorescence values were normalized to the first time point following photoactivation and averaged from different cells for each time point. The kinetics of fluorescence loss after activation were fit to a double exponential curve, and regression analysis was performed as described previously [19–21, 25] with Origin 6 software (OriginLab).

Spindle Structure Analysis

Spindle length from prometaphase or metaphase HeLa cells was calculated with NIH ImageJ software by measuring the distance between spindle poles in 3D. CLASP1 or CENP-E staining at the poles was used as a reference. Assays for analysis of bipolar spindle formation after siRNA depletion of the indicated proteins were performed as described previously [32].

Supplemental Data

Supplemental Data include eight figures, one table, and one movie and can be found with this article online at [http://www.cell.com/current-biology/supplemental/S0960-9822\(09\)01485-7](http://www.cell.com/current-biology/supplemental/S0960-9822(09)01485-7).

Acknowledgments

We thank I. Cheeseman for guidance and providing reagents for LAP purifications; A.J. Pereira and S. Bakhom for development of MATLAB routines used in this paper and advice on the quantification of microtubule dynamics parameters; P. Sampaio for assistance with photoactivation; and A. Akhmanova, T. Yen, and W. Earnshaw for generous gifts of reagents. S.M., A.R.R.M., and A.L.P. hold fellowships from the Fundação para a Ciência e a Tecnologia (FCT) of Portugal (SFRH/BPD/26780/2006; SFRH/BD/32976/2006; SFRH/BD/25084/2005). Work in the laboratory of D.A.C. is supported by National Institutes of Health grant GM51542. Work in the laboratory of H.M. is supported by grants PTDC/BIA-BCM/66106/2006 and PTDC/SAU-OB/66113/2006 from FCT and the Gulbenkian Programme on the Frontiers in Life Sciences.

Received: May 14, 2009

Revised: July 9, 2009

Accepted: July 22, 2009

Published online: September 3, 2009

References

- Cheeseman, I.M., and Desai, A. (2008). Molecular architecture of the kinetochore-microtubule interface. *Nat. Rev. Mol. Cell Biol.* 9, 33–46.
- Maiato, H., Fairley, E.A., Rieder, C.L., Swedlow, J.R., Sunkel, C.E., and Earnshaw, W.C. (2003). Human CLASP1 is an outer kinetochore component that regulates spindle microtubule dynamics. *Cell* 113, 891–904.
- Maiato, H., Khodjakov, A., and Rieder, C.L. (2005). Drosophila CLASP is required for the incorporation of microtubule subunits into fluxing kinetochore fibres. *Nat. Cell Biol.* 7, 42–47.
- Pereira, A.L., Pereira, A.J., Maia, A.R., Drabek, K., Sayas, C.L., Hergert, P.J., Lince-Faria, M., Matos, I., Duque, C., Stepanova, T., et al. (2006). Mammalian CLASP1 and CLASP2 cooperate to ensure mitotic fidelity by regulating spindle and kinetochore function. *Mol. Biol. Cell* 17, 4526–4542.
- Wood, K.W., Sakowicz, R., Goldstein, L.S., and Cleveland, D.W. (1997). CENP-E is a plus end-directed kinetochore motor required for metaphase chromosome alignment. *Cell* 91, 357–366.
- Cheeseman, I.M., and Desai, A. (2005). A combined approach for the localization and tandem affinity purification of protein complexes from metazoans. *Sci. STKE* 2005, pl1.
- Akhmanova, A., Hoogenraad, C.C., Drabek, K., Stepanova, T., Dortmund, B., Verkerk, T., Vermeulen, W., Burgering, B.M., De Zeeuw, C.I., Grosveld, F., and Galjart, N. (2001). Clasps are CLIP-115 and -170 associating proteins involved in the regional regulation of microtubule dynamics in motile fibroblasts. *Cell* 104, 923–935.
- Lansbergen, G., Grigoriev, I., Mimori-Kiyosue, Y., Ohtsuka, T., Higa, S., Kitajima, I., Demmers, J., Galjart, N., Houtsmuller, A.B., Grosveld, F., and Akhmanova, A. (2006). CLASPs attach microtubule plus ends to the cell cortex through a complex with LL5beta. *Dev. Cell* 11, 21–32.
- Efimov, A., Kharitonov, A., Efimova, N., Loncarek, J., Miller, P.M., Andreyeva, N., Gleeson, P., Galjart, N., Maia, A.R., McLeod, I.X., et al. (2007). Asymmetric CLASP-dependent nucleation of noncentrosomal microtubules at the trans-Golgi network. *Dev. Cell* 12, 917–930.
- Hannak, E., and Heald, R. (2006). Xorbit/CLASP links dynamic microtubules to chromosomes in the *Xenopus* meiotic spindle. *J. Cell Biol.* 172, 19–25.
- Delgehyr, N., Sillibourne, J., and Bornens, M. (2005). Microtubule nucleation and anchoring at the centrosome are independent processes linked by ninein function. *J. Cell Sci.* 118, 1565–1575.
- Kleylein-Sohn, J., Westendorf, J., Le Clech, M., Habedanck, R., Stierhof, Y.D., and Nigg, E.A. (2007). Plk4-induced centriole biogenesis in human cells. *Dev. Cell* 13, 190–202.
- Drewes, G., Ebnet, A., Preuss, U., Mandelkow, E.M., and Mandelkow, E. (1997). MARK, a novel family of protein kinases that phosphorylate microtubule-associated proteins and trigger microtubule disruption. *Cell* 89, 297–308.
- Cooke, C.A., Schaar, B., Yen, T.J., and Earnshaw, W.C. (1997). Localization of CENP-E in the fibrous corona and outer plate of mammalian kinetochores from prometaphase through anaphase. *Chromosoma* 106, 446–455.
- Cheeseman, I.M., MacLeod, I., Yates, J.R., 3rd, Oegema, K., and Desai, A. (2005). The CENP-F-like proteins HCP-1 and HCP-2 target CLASP to kinetochores to mediate chromosome segregation. *Curr. Biol.* 15, 771–777.
- Bomont, P., Maddox, P., Shah, J.V., Desai, A.B., and Cleveland, D.W. (2005). Unstable microtubule capture at kinetochores depleted of the centromere-associated protein CENP-F. *EMBO J.* 24, 3927–3939.
- Schaar, B.T., Chan, G.K., Maddox, P., Salmon, E.D., and Yen, T.J. (1997). CENP-E function at kinetochores is essential for chromosome alignment. *J. Cell Biol.* 139, 1373–1382.
- Henderson, M.C., Shaw, Y.J., Wang, H., Han, H., Hurley, L.H., Flynn, G., Dorr, R.T., and Von Hoff, D.D. (2009). UA62784, a novel inhibitor of centromere protein E kinesin-like protein. *Mol. Cancer Ther.* 8, 36–44.
- Zhai, Y., Kronebusch, P.J., and Borisy, G.G. (1995). Kinetochore microtubule dynamics and the metaphase-anaphase transition. *J. Cell Biol.* 131, 721–734.

20. Cimini, D., Wan, X., Hirel, C.B., and Salmon, E.D. (2006). Aurora kinase promotes turnover of kinetochore microtubules to reduce chromosome segregation errors. *Curr. Biol.* *16*, 1711–1718.
21. Bakhom, S.F., Thompson, S.L., Manning, A.L., and Compton, D.A. (2009). Genome stability is ensured by temporal control of kinetochore-microtubule dynamics. *Nat. Cell Biol.* *11*, 27–35.
22. Ganem, N.J., Upton, K., and Compton, D.A. (2005). Efficient mitosis in human cells lacking poleward microtubule flux. *Curr. Biol.* *15*, 1827–1832.
23. Maiato, H., Sampaio, P., Lemos, C.L., Findlay, J., Carmena, M., Earnshaw, W.C., and Sunkel, C.E. (2002). MAST/Orbit has a role in microtubule-kinetochore attachment and is essential for chromosome alignment and maintenance of spindle bipolarity. *J. Cell Biol.* *157*, 749–760.
24. Mimori-Kiyosue, Y., Grigoriev, I., Sasaki, H., Matsui, C., Akhmanova, A., Tsukita, S., and Vorobjev, I. (2006). Mammalian CLASPs are required for mitotic spindle organization and kinetochore alignment. *Genes Cells* *11*, 845–857.
25. DeLuca, J.G., Gall, W.E., Ciferri, C., Cimini, D., Musacchio, A., and Salmon, E.D. (2006). Kinetochore microtubule dynamics and attachment stability are regulated by Hec1. *Cell* *127*, 969–982.
26. McEwen, B.F., Chan, G.K., Zubrowski, B., Savoian, M.S., Sauer, M.T., and Yen, T.J. (2001). CENP-E is essential for reliable bioriented spindle attachment, but chromosome alignment can be achieved via redundant mechanisms in mammalian cells. *Mol. Biol. Cell* *12*, 2776–2789.
27. Putkey, F.R., Cramer, T., Morphew, M.K., Silk, A.D., Johnson, R.S., McIntosh, J.R., and Cleveland, D.W. (2002). Unstable kinetochore-microtubule capture and chromosomal instability following deletion of CENP-E. *Dev. Cell* *3*, 351–365.
28. Cheeseman, I.M., Chappie, J.S., Wilson-Kubalek, E.M., and Desai, A. (2006). The conserved KMN network constitutes the core microtubule-binding site of the kinetochore. *Cell* *127*, 983–997.
29. Hoffman, D.B., Pearson, C.G., Yen, T.J., Howell, B.J., and Salmon, E.D. (2001). Microtubule-dependent changes in assembly of microtubule motor proteins and mitotic spindle checkpoint proteins at Ptk1 kinetochores. *Mol. Biol. Cell* *12*, 1995–2009.
30. Manning, A.L., Ganem, N.J., Bakhom, S.F., Wagenbach, M., Wordeman, L., and Compton, D.A. (2007). The kinesin-13 proteins Kif2a, Kif2b, and Kif2c/MCAK have distinct roles during mitosis in human cells. *Mol. Biol. Cell* *18*, 2970–2979.
31. Cassimeris, L., Becker, B., and Carney, B. (2009). TOGp regulates microtubule assembly and density during mitosis and contributes to chromosome directional instability. *Cell Motil. Cytoskeleton* *66*, 535–545.
32. Ganem, N.J., and Compton, D.A. (2004). The KinI kinesin Kif2a is required for bipolar spindle assembly through a functional relationship with MCAK. *J. Cell Biol.* *166*, 473–478.
33. Laycock, J.E., Savoian, M.S., and Glover, D.M. (2006). Antagonistic activities of Klp10A and Orbit regulate spindle length, bipolarity and function in vivo. *J. Cell Sci.* *119*, 2354–2361.
34. Buster, D.W., Zhang, D., and Sharp, D.J. (2007). Poleward tubulin flux in spindles: Regulation and function in mitotic cells. *Mol. Biol. Cell* *18*, 3094–3104.
35. Lombillo, V.A., Nislow, C., Yen, T.J., Gelfand, V.I., and McIntosh, J.R. (1995). Antibodies to the kinesin motor domain and CENP-E inhibit microtubule depolymerization-dependent motion of chromosomes in vitro. *J. Cell Biol.* *128*, 107–115.
36. Kapoor, T.M., Lampson, M.A., Hergert, P., Cameron, L., Cimini, D., Salmon, E.D., McEwen, B.F., and Khodjakov, A. (2006). Chromosomes can congress to the metaphase plate before biorientation. *Science* *311*, 388–391.
37. Abrieu, A., Kahana, J.A., Wood, K.W., and Cleveland, D.W. (2000). CENP-E as an essential component of the mitotic checkpoint in vitro. *Cell* *102*, 817–826.
38. Mao, Y., Desai, A., and Cleveland, D.W. (2005). Microtubule capture by CENP-E silences BubR1-dependent mitotic checkpoint signaling. *J. Cell Biol.* *170*, 873–880.
39. Yao, X., Abrieu, A., Zheng, Y., Sullivan, K.F., and Cleveland, D.W. (2000). CENP-E forms a link between attachment of spindle microtubules to kinetochores and the mitotic checkpoint. *Nat. Cell Biol.* *2*, 484–491.
40. Lampson, M.A., and Kapoor, T.M. (2005). The human mitotic checkpoint protein BubR1 regulates chromosome-spindle attachments. *Nat. Cell Biol.* *7*, 93–98.
41. Maia, A.F., Lopes, C.S., and Sunkel, C.E. (2007). BubR1 and CENP-E have antagonistic effects upon the stability of microtubule-kinetochore attachments in *Drosophila* S2 cell mitosis. *Cell Cycle* *6*, 1367–1378.
42. Ditchfield, C., Johnson, V.L., Tighe, A., Ellston, R., Haworth, C., Johnson, T., Mortlock, A., Keen, N., and Taylor, S.S. (2003). Aurora B couples chromosome alignment with anaphase by targeting BubR1, Mad2, and Cenp-E to kinetochores. *J. Cell Biol.* *161*, 267–280.
43. Poser, I., Sarov, M., Hutchins, J.R., Hériché, J.K., Toyoda, Y., Pozniakovskiy, A., Weigl, D., Nitzsche, A., Hegemann, B., Bird, A.W., et al. (2008). BAC TransgeneOmics: A high-throughput method for exploration of protein function in mammals. *Nat. Methods* *5*, 409–415.
44. Harborth, J., Elbashir, S.M., Bechert, K., Tuschl, T., and Weber, K. (2001). Identification of essential genes in cultured mammalian cells using small interfering RNAs. *J. Cell Sci.* *114*, 4557–4565.
45. DeLuca, J.G., Moree, B., Hickey, J.M., Kilmartin, J.V., and Salmon, E.D. (2002). hNuf2 inhibition blocks stable kinetochore-microtubule attachment and induces mitotic cell death in HeLa cells. *J. Cell Biol.* *159*, 549–555.
46. Mimori-Kiyosue, Y., Grigoriev, I., Lansbergen, G., Sasaki, H., Matsui, C., Severin, F., Galjart, N., Grosveld, F., Vorobjev, I., Tsukita, S., and Akhmanova, A. (2005). CLASP1 and CLASP2 bind to EB1 and regulate microtubule plus-end dynamics at the cell cortex. *J. Cell Biol.* *168*, 141–153.
47. Link, A.J., Eng, J., Schieltz, D.M., Carmack, E., Mize, G.J., Morris, D.R., Garvik, B.M., and Yates, J.R., 3rd. (1999). Direct analysis of protein complexes using mass spectrometry. *Nat. Biotechnol.* *17*, 676–682.